

1 **Atypical beta-band effects in children with dyslexia in response to rhythmic**
2 **audio-visual speech**

3

4

5 Mahmoud Keshavarzi*, Kanad Mandke, Annabel Macfarlane, Lyla Parvez, Fiona Gabrielczyk,

6 Angela Wilson, Usha Goswami

7

8 *Centre for Neuroscience in Education, Department of Psychology, University of Cambridge,*

9 *Cambridge, CB2 3EB, United Kingdom*

10

11

12

13

14 *Correspondence to: mk919@cam.ac.uk, mahmoud.keshavarzi.ir@ieee.org

15 **Abstract**

16 Children with dyslexia are known to show impairments in perceiving speech rhythm, which impact
17 their phonological development. Neural rhythmic speech studies have reported atypical delta phase
18 in children with dyslexia, but beta band effects have not yet been studied. It is known that delta
19 phase modulates the amplitude of the beta band response during rhythmic tasks via delta-beta
20 phase-amplitude coupling (PAC). Accordingly, the atypical delta band effects reported for children
21 with dyslexia may imply related atypical beta band effects. Here we analyse EEG data collected
22 during a rhythmic speech paradigm from 51 children (21 typically-developing; 30 with dyslexia)
23 who attended to a talking head repeating “ba” at 2Hz. Phase entrainment in the beta band, angular
24 velocity in the beta band, power responses in the beta band and delta-beta PAC were assessed for
25 each child and each group. Phase entrainment in the beta band was only significant for children
26 without dyslexia. Children with dyslexia did not exhibit any phase consistency, and beta-band
27 angular velocity was significantly faster compared to control children. Power in the beta band was
28 significantly greater in the children with dyslexia. Delta-beta PAC was significant in both groups.
29 The data are interpreted with respect to temporal sampling theory.

30

31 **Keywords**

32 Developmental dyslexia, phase entrainment, phase-amplitude coupling, beta band, rhythmic
33 audio-visual speech.

34 **1. Introduction**

35 There is an intimate developmental relationship between rhythmic skills and language
36 development, and this relationship has been documented by behavioural studies in a range of
37 languages (Fiveash et al., 2021, for recent review). Infants appear to begin the task of language-
38 learning by utilising speech rhythm (Mehler et al., 1988), and linguistic analyses propose that
39 languages can be divided into specific rhythm types (stress-timed, syllable-timed, moraic timing)
40 which are already perceived as different by newborn infants (Nazzi et al., 1998). Indeed,
41 computational modelling of infant-directed speech (IDS) shows that IDS has extra modulation
42 energy in the delta band in the speech amplitude envelope compared to adult-directed speech,
43 which serves perceptually to exaggerate rhythmic structure (Leong et al., 2017). Further, delta-
44 band entrainment to rhythmic speech is significantly stronger than theta-band entrainment for
45 infants aged 4, 7 and 11 months, and individual differences in delta-band cortical tracking at 11
46 months predict language outcomes at 24 months (Attaheri et al., 2022, 2023). The ubiquitous role
47 of rhythm in language acquisition has led to the proposal that atypical rhythm skills in infancy and
48 early childhood may be a core factor in the development of language disorders such as
49 developmental dyslexia and developmental language disorder (DLD, Ladányi et al., 2020).
50 Children with developmental dyslexia typically present with phonological difficulties relating to
51 the sound structure of speech, while children with DLD present with grammatical impairments. At
52 the sensory/neural level, this ‘atypical rhythm risk hypothesis’ is captured by Temporal Sampling
53 (TS) theory (Goswami, 2011; 2015, 2022), which is focused on automatic processing of the speech
54 amplitude envelope (AE).

55 TS theory suggests that difficulties in rhythm perception and production in infancy and
56 childhood arise from atypical sensory/neural processing of the lower frequency portion (<10 Hz)

57 of the AE, the slow-varying energy contour of speech which determines the perception of speech
58 rhythm (Greenberg, 2006). Regarding the sensory aspects of TS theory, there are known to be
59 different rates of amplitude modulation (AM) nested in the speech envelope centred on ~2 Hz, ~5
60 Hz and ~20 Hz (Leong and Goswami, 2015), and research has shown that rates <10 Hz are those
61 most critical for perceiving rhythm (Greenberg, 2003, 2006). Speech modelling of the AE (of IDS
62 and nursery rhymes) has revealed that the *phase relations* between these different AM rates nested
63 in the envelope (which approximately match the EEG bands of delta [0.5-4 Hz], theta [4-8 Hz],
64 and beta/ low gamma [12-40 Hz] for child speech) provide systematic statistical clues to
65 phonological units in speech (Leong et al., 2017; Leong and Goswami, 2015). Accordingly,
66 difficulties in perceiving and encoding the different rates of AM nested in the speech AE and their
67 phase relations could impair automatic statistical learning about the phonological structure of the
68 speech signal for children with dyslexia. Computational analyses show that AM cycles at these 3
69 temporal rates (delta, theta, beta/low gamma) support the extraction of stressed vs unstressed
70 syllable patterning (speech prosody), syllables, and onset-rimes respectively (‘acoustic-emergent
71 phonology’, see Leong and Goswami, 2015). Children with dyslexia show impaired discrimination
72 of amplitude rise times and AM across languages (Goswami, 2022, for recent review). The
73 cognitive hallmark of developmental dyslexia is the “phonological core deficit” (Stanovich, 1988),
74 defined by children’s reduced ability to identify and manipulate phonological units like syllables,
75 rhymes and phonemes in oral tasks. By TS theory, this core phonological deficit arises in part from
76 inefficient sensory discrimination of amplitude rise times and AMs.

77 Regarding the neural side of TS theory, MEG studies of children with dyslexia using story
78 listening tasks suggest that the neural encoding impairments regarding speech information lie
79 primarily in the encoding of low-frequency envelope information (Molinaro et al., 2016: Spanish;

80 Mandke et al., 2022: English; Destoky et al., 2020; French). EEG studies assessing speech
81 encoding mechanisms by using linear methods for measuring neural encoding such as temporal
82 response functions (TRFs) suggest that children with dyslexia show atypical neural encoding of
83 continuous speech in the delta band (Power et al., 2016; Di Liberto et al., 2018; Keshavarzi et al.,
84 2022b). Potential differences between children with and without dyslexia in the neural phase of
85 oscillation for delta, theta and alpha bands have been assessed by utilising rhythmic speech
86 paradigms (such as repetition of the syllable ‘ba’ at 2 Hz; Power et al., 2012, 2013; Keshavarzi et
87 al., 2022a). These latter EEG studies suggest that one core neural problem during speech
88 processing relates to inaccurate phase synchronisation of the cortical networks that respond to
89 delta-band AM information in the speech signal (Goswami, 2022, for a recent review). If the
90 dyslexic brain is “out of phase” in its response to speech information in the delta band, then this
91 might affect the accuracy of neural processing of the entire AM hierarchy nested in the speech
92 signal, and thereby the extraction of phonology. This follows because neural responses to natural
93 speech exhibit a mechanistic hierarchy governed by the delta band, in which phase relations and
94 phase-amplitude relations between different frequency bands are utilised to capture the full
95 complexity of the sensory information in speech (Gross et al., 2013; Ding and Simon, 2014;
96 Doelling et al., 2014). For example, delta-beta PAC is thought to underpin temporal prediction
97 accuracy during rhythmic processing via sensory-motor coupling (Arnal and Giraud, 2012; Arnal
98 et al., 2015). Delta-beta PAC is already online in 4-month-old infants during speech listening
99 (Attaheri et al., 2022), and is known to play a role in natural speech processing in the adult brain
100 (Keitel et al., 2018). A prior study of children with dyslexia using a sentence listening task found
101 intact delta-beta PAC (Power et al., 2016). Accordingly, atypical phase in the delta band might not

102 necessarily be expected to attenuate delta-beta PAC, however this has yet to be investigated in
103 rhythmic tasks.

104 Despite its potential importance for accurate rhythmic processing, the beta band has been
105 relatively neglected in developmental language studies using EEG. However, recent longitudinal
106 research in Mandarin Chinese based on resting-state EEG has shown that beta power increases
107 over time between the ages of 7 and 11 years, and that the degree of increase in beta power from
108 age 7 to 9 years predicts vocabulary at age 11 years (Meng et al., 2021). This relationship is
109 significant even after controlling for cognitive ability, SES and home literacy environment (Meng
110 et al., 2021). A role for the beta band in linguistic development may be consistent with adult data,
111 as the magnitude of beta oscillatory responses in the adult brain has been associated with both
112 speech comprehension and with predictive coding of speech (Gisladottir et al., 2018). Regarding
113 beta band studies including children with dyslexia, a study of German children with and without
114 developmental dyslexia found some group differences in beta-band power when the children were
115 reading single words or pseudowords aloud (Klimesch et al., 2001). In particular, Klimesch and
116 colleagues reported greater power in a narrow beta band range (12-14 Hz) in frontal, right central
117 and centroparietal regions during pseudoword reading by children with dyslexia. However, the
118 authors noted that the functional significance of this power increase was difficult to ascertain.
119 Working in Italian, Spironelli et al. (2008) also reported greater beta-band power in children with
120 dyslexia, both during a phonological task (judging whether two written words rhymed) and a
121 semantic task (judging whether two written words were semantically related). Accordingly,
122 developmental data suggest an involvement of beta power in various linguistic tasks delivered via
123 print. More recently, Power et al. (2016) reported greater beta power in children with dyslexia
124 compared to age-matched control children during a sentence listening task where no print was

125 involved. In a word recognition task conducted with adults with dyslexia involving print (lexical
126 decision task), Milne et al. (2003) recorded EEG while participants decided whether letter strings
127 were words or not. They also reported higher beta power for dyslexic adults compared to non-
128 dyslexic adults. Finally, in a recent EEG study with dyslexic adults using a beat perception task
129 (participants listened to isochronous tones presented at a 2 Hz rate), Chang et al. (2021) reported
130 that fluctuations in beta power differed between dyslexic and control adults. This was interpreted
131 to reflect behavioural deficits in perceiving and tracking auditory rhythm in dyslexia, as would be
132 predicted by TS theory.

133 Phase entrainment in the beta band has yet to be explored in children with dyslexia in a
134 beat-based task. Accordingly, here we re-analyse the EEG data reported by Keshavarzi et al.
135 (2022a), which investigated the delta, theta and alpha bands, this time focusing on the beta band.
136 The EEG was recorded while children aged 9 years with and without dyslexia listened to the speech
137 syllable “ba” presented rhythmically at a rate of 2 Hz. Given that the participating children with
138 dyslexia had already shown less consistent phase entrainment in the delta band (Keshavarzi et al.,
139 2022a) and given that delta phase couples with beta amplitude via delta-beta PAC (see also Arnal
140 et al., 2014), group differences (in terms of phase entrainment, angular velocity, and beta power)
141 in the beta band might be expected. We thus also computed delta-beta PAC, beta power and
142 angular velocity in the beta band for our children. In the delta band analyses conducted with the
143 same children, Keshavarzi et al. (2022a) reported a significantly greater angular velocity in
144 children with dyslexia compared to control children over a time interval of –130 ms to 0 ms. This
145 was taken to indicate that pre-stimulus delta phase was different in the two groups. If the phase of
146 beta entrainment is atypical in the dyslexic brain, angular velocity in the beta band may also be
147 expected to differ by group.

148 **2. Method**

149 *2.1. Participants*

150 Thirty children with developmental dyslexia (mean age = 110.7 months; SD = 5.6 months) and
151 twenty-one typically developing children (mean age = 109.3 months; SD = 5.4 months) took part
152 in the EEG study. The children were identified as dyslexic or typically-developing based on
153 standardized reading, spelling and phonological awareness tests administered in 2018 (please see
154 Keshavarzi et al., 2022a, for full details). They were assessed using the British Ability Scales
155 standardized tests of reading and spelling (Elliott et al., 1996), the Test of Word Reading Efficiency
156 word and nonword scales (TOWRE, Torgesen et al., 1999), and the rhyming subtest of the
157 Phonological Assessment Battery (PhAB, Frederickson et al., 1997). Only children who scored at
158 least one standard deviation below the test norm of 100 on at least two of the four reading and
159 spelling measures and/or the phonology measure were included in the study. A summary of
160 performance by group is shown as Table 1. Dyslexic children had no additional learning issues
161 (e.g., dyspraxia, ADHD, autistic spectrum disorder, developmental language disorder) and were
162 recruited through learning support teachers. They had a nonverbal IQ above 84, and English was
163 their first language spoken at home. The absence of additional learning difficulties was assessed
164 based on school and parental reports and our own testing impressions. Participants were attending
165 state schools (equivalent to US public schools) situated in a range of towns and villages near a
166 university town in the United Kingdom. Most families were Caucasian and of lower class or
167 middle-class regarding income. All children received a short hearing screen using an audiometer.
168 Sounds were presented in both the left and right ear at a range of frequencies (250, 500, 1000,
169 2000, 4000, 8000Hz), and all children were sensitive to sounds within the 20 dB HL range.

170

171 **Table 1.** Group characteristics expressed as mean and (S.D.) for children with dyslexia and age-
172 matched control children on the reading, spelling and phonological measures.

	Dyslexic	Age-Matched Control
N	30	21
Age (months)	110.7 (5.6)	109.3 (5.4)
BAS Reading SS	81.0 (8.0) ***	99.5 (6.2)
BAS Reading Age in months	85.5 (11.0) ***	106.5 (11.7)
BAS Spelling SS	79.9 (7.5) ***	97.1 (6.1)
TOWRE SWE SS	79.5 (12.8) ***	101.1 (7.7)
TOWRE PDE SS	79.2 (10.9) ***	98.0 (8.6)
PhAB Rhyme SS	92.6 (11.7) ***	102.4 (5.9)

173 Note. *** $p < .001$. BAS = British Ability Scales; SS = standardized score (mean = 100); TOWRE SWE =
174 Test of Word Reading Efficiency Sight Word Efficiency Scale; TOWRE PDE = Phonic Decoding
175 Efficiency Scale; PhAB = Phonological Assessment Battery.

176

177 2.2. Experimental paradigm and stimuli

178 The experimental paradigm and stimuli were exactly as described by Keshavarzi et al. (2022a).

179 The stimuli comprised of rhythmic sequences of the syllable “ba” repeating 14 times at a rate of 2

180 Hz. One of the 14 “ba” syllables (at either position 9, 10 or 11) in each sequence was randomly

181 out of time. Each child was presented with 90 trials, 15 of which were catch trials which were

182 presented randomly and did not contain a lagged syllable. Each trial (except catch trials) consisted

183 of three periods: the entrainment period (including syllables 1 – 8, 1 – 9 or 1–10 depending on the

184 position of the lagged syllable), the violation period (including syllables 9 – 10, 10 – 11 or 11 – 12

185 depending on the position of the lagged syllable) and the return-to-isochrony period (including

186 syllables 11 – 14, 12 – 14 or 13 – 14 depending on the position of the lagged syllable). Figure 1

187 illustrates an example of a trial with the lagged syllable at position 10. There was a fixed time

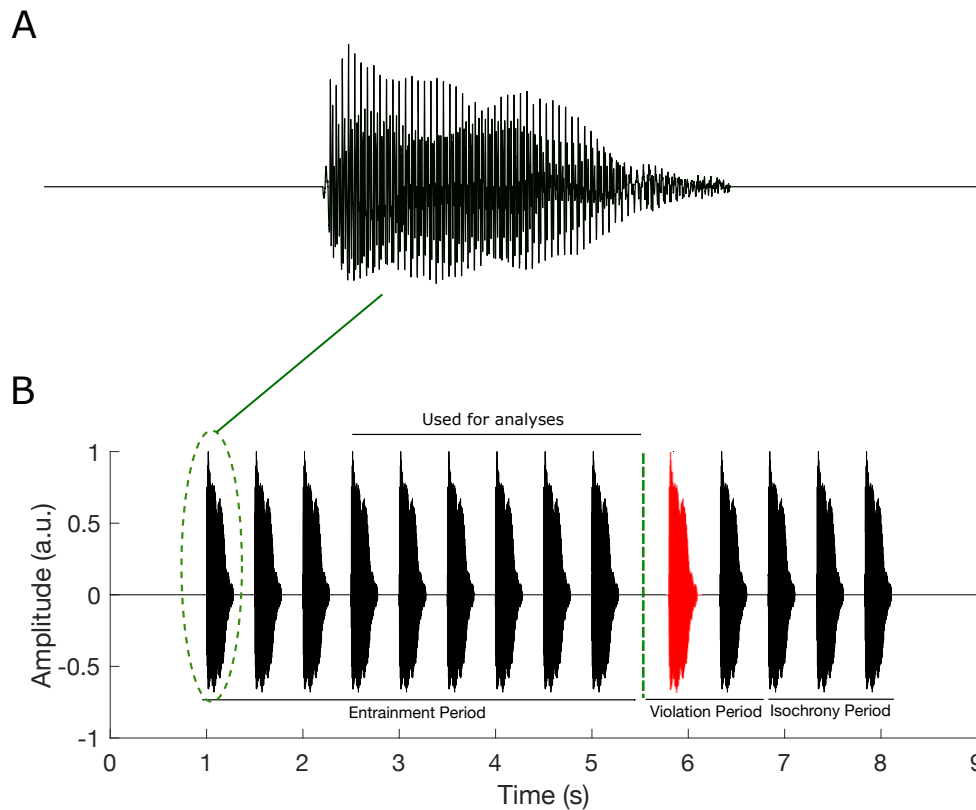
188 interval of 500 ms between successive “ba” stimuli in the entrainment period. The extent to which

189 the violator was out of the isochronous rhythm varied depending on how well the child responded

190 in the task and followed a 3-down 1-up staircase procedure (Levitt, 1971). If a child correctly

191 detected the violators in three successive trials, then the deviation from 500 ms stimulus-onset

192 asynchrony decreased by 16.67 ms. If a violator was not detected, the deviation increased by 16.67
193 ms. There was a 3 second interval between successive trials.



194

195 **Figure 1. Experimental stimuli. Figure reproduced with permission from Keshavarzi et al.,**
196 **2022a. (A) waveform of a single auditory “ba”, (B) a sequence of “ba” with the oddball as**
197 **stimulus 10.** The auditory stimuli consisted of the syllable “ba” repeated 14 times per trial at a rate
198 of 2 Hz, with one syllable of stimuli 9-11 being out of the rhythm (here syllable 10, depicted in
199 red). For this example (panel B), stimuli 4-9 of the entrainment period were used for the analysis.
200

201 2.3. EEG Data Acquisition

202 Participants were seated in a soundproof chamber. The auditory stimuli and visual speech
203 information were presented to the participant and EEG data were simultaneously collected at 1-
204 kHz sampling rate using a 128-channel EEG system (HydroCel Geodesic Sensor Net). Visual cues
205 started 68 ms before the onset of the auditory stimulus “ba” as in natural speech. Children were
206 instructed to focus on the lips of the talking face and to listen to the auditory stimuli. They also

207 were asked to press a target key on the computer keyboard if one of the syllables was out of time.
208 The EEG study (excluding the EEG set-up and preparation) took approximately 15 minutes.

209 *2.5. EEG Data Pre-processing*

210 The EEG pre-processing applied in this study is the same as the one described by Keshavarzi et
211 al. (2022a). After considering the Cz channel as the reference, a zero phase FIR filter with a low
212 cutoff (-6 dB) of 0.25 Hz and high cutoff (-6 dB) of 48.25 Hz (EEGLab Toolbox; Delorme and
213 Makeig, 2004) was used to band-passed filter data at frequency range of 0.5 – 48 Hz. We detected
214 extremely noisy channels using the spectrogram, kurtosis and probability methods provided by
215 EEGLAB Toolbox. If a channel was 3 S.D. away from the average, it was rejected and interpolated
216 using spherical interpolation (EEGLab Toolbox). We applied the independent component analysis,
217 provided in EEGLab Toolbox, to the data for each participant. The obtained independent
218 components were then assessed carefully to remove artefactual components such as eye
219 movements. Participant head movements during the EEG recording were monitored using a
220 camera installed in the EEG room and the times corresponding to head movements were manually
221 recorded by the experimenter. This information was then used to ensure that trials corrupted by
222 head movements had been cleaned by the pre-processing steps. The EEG data were downsampled
223 to 100 Hz and band-pass filtered to extract delta (0.5 – 4 Hz) and beta (15 – 25 Hz) frequency
224 bands. The data were then epoched into individual trials, in the time range of 500 ms before the
225 onset of the first stimulus and 4.5 sec after that. Some trials were excluded from the analyses
226 because of technical issues such as stimulus information not being marked in the EEG file. The
227 average number of trials utilised for the analyses for control and dyslexic groups were 77.61 (S.D.
228 = 20.01) and 78.13 (S.D. = 21.67), respectively. We obtained the instantaneous phase separately
229 for each EEG channel (filtered at the beta band) using two steps: (1) Computing the analytic

230 representation of the input signal through the Hilbert transform; (2) Computing the phase of each
231 sample (which is a complex value) of the analytic signal. Note that the focus of the analyses in this
232 study was only on the entrainment period. To ensure that rhythmicity had been established and to
233 maximise data, we excluded the first two “ba” stimuli for trials with a violation occurring at
234 position 9 (hence our analyses used stimuli 3 – 8) and the first three “ba” stimuli for trials where
235 the violation occurred at position either 10 or 11 (hence our analyses used stimuli 4 – 9). This
236 resulted in a maximum of 540 “ba” stimuli for each participant.

237 *2.7. Computation of phase entrainment*

238 To assess the phase entrainment for each group in the beta band, the following six steps were
239 performed (as previously used by Keshavarzi et al. (2022a) for investigating delta, theta and alpha):

- 240 • Step 1. Calculating instantaneous phases of all 128 EEG channels at the times corresponding
241 to the onsets of the 6 “ba” stimuli that were used for the analyses for each of the 90 trials.
- 242 • Step 2. Calculating the mean phase for each of the 90 trials by averaging across the phase
243 observations obtained for 128 EEG channels and for the 6 “ba” stimuli in step 1. This results
244 in a single-phase value for each trial.
- 245 • Step 3. Deriving a single unit vector (whose angle is determined by the phase value obtained
246 in step 2) in the vector space for each trial.
- 247 • Step 4. Calculating the mean vector for each child by averaging across the unit vectors obtained
248 in step 3. This results in a single vector for each child, subsequently we refer to this as the *child*
249 *resultant vector*. The length of the *child resultant vector* is a value between 0 and 1 and its
250 angle, called *child preferred phase*, is between 0 and 2π . The length of the *child resultant*
251 *vector* can be used as a criterion to assess the strength of phase consistency across different
252 trials for each individual participant.

- 253 • Step 5. A single unit vector (whose angle is determined by the *child preferred phase* obtained
254 in step 4) is considered in the vector space for each child.
- 255 • Step 6. The mean vector for each group is computed by averaging across the unit vectors
256 obtained in step 5. This produces a single vector, called the *group resultant vector*, for each
257 group. The length of the *group resultant vector* is a value between 0 and 1 and its angle, called
258 *group preferred phase*, is between 0 and 2π . The length of the *group resultant vector* can be
259 used as a criterion to assess the strength of phase consistency across different children by
260 group.

261 2.8. Computation of phase-amplitude coupling

262 Phase amplitude coupling (PAC) refers to a type of cross-frequency coupling in which the
263 amplitude of the signal at a high-frequency band is modulated by the phase of low-frequency
264 oscillations. In this study, we quantified the strength of this modulation using the modulation
265 index (*MI*; Tort et al. 2008; Hülsemann, 2019):

$$266 \quad MI = \frac{KL(U,X)}{\log B} \quad (1)$$

267 where $B (=18)$ is the number of bins, U refers to the uniform distribution, X is the distribution of
268 the data, and $KL(U,X)$ is Kullback–Leibler distance, a measure of the disparity of two
269 distributions (Hülsemann, 2019), and is calculated by:

$$270 \quad KL(U,X) = \log B - H(P) \quad (2)$$

271 where $H(\cdot)$ is the Shannon entropy and P is the vector of normalized averaged amplitudes per
272 phase bin which is calculated as:

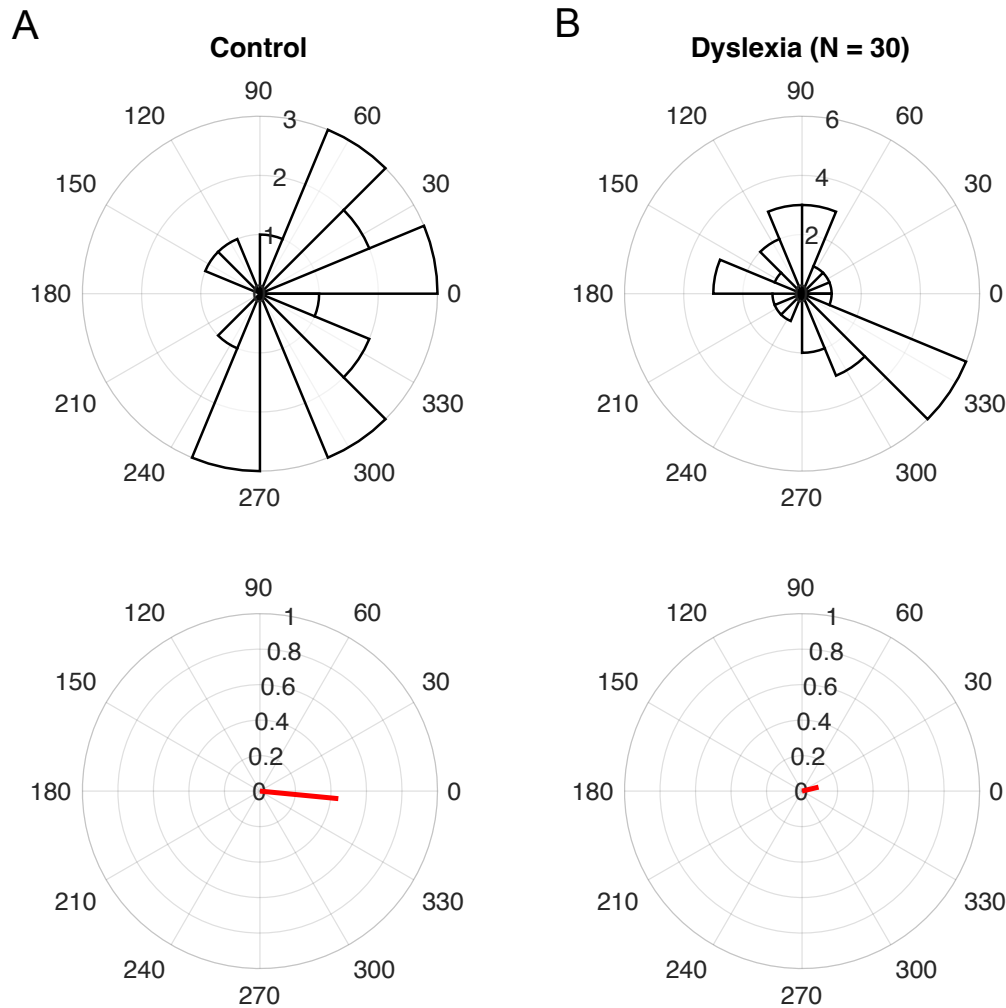
$$273 \quad P(j) = \frac{\bar{a}}{\sum_{k=1}^N \bar{a}_k} \quad , \quad j = 1, \dots, N \quad (3)$$

274 where \bar{a} is the average amplitude of each bin and k refers to running index for the bins. Note that
275 P is a vector with N elements.

276 **3. Results**

277 *3.1. Phase entrainment in the beta band within each group*

278 To check the consistency of phase entrainment across the different children in each group, the
279 Rayleigh test of uniformity was applied to the *child preferred phases* (angles of *child resultant*
280 *vectors*, see step 4 in subsection 2.7) separately for each group. The distribution of phase at the
281 onsets of the “ba” stimuli was significantly different from the uniform distribution for the control
282 children (Rayleigh test, $z = 4.13$, $p = 0.01$; see Figure 2A), indicating consistent phase entrainment.
283 For children with dyslexia, however, the distribution of phase at the onsets of the “ba” stimuli did
284 not differ from the uniform distribution (Rayleigh test, $z = 0.27$, $p = 0.76$; see Figure 2B),
285 suggesting that consistent phase entrainment was not present in the beta band.



286

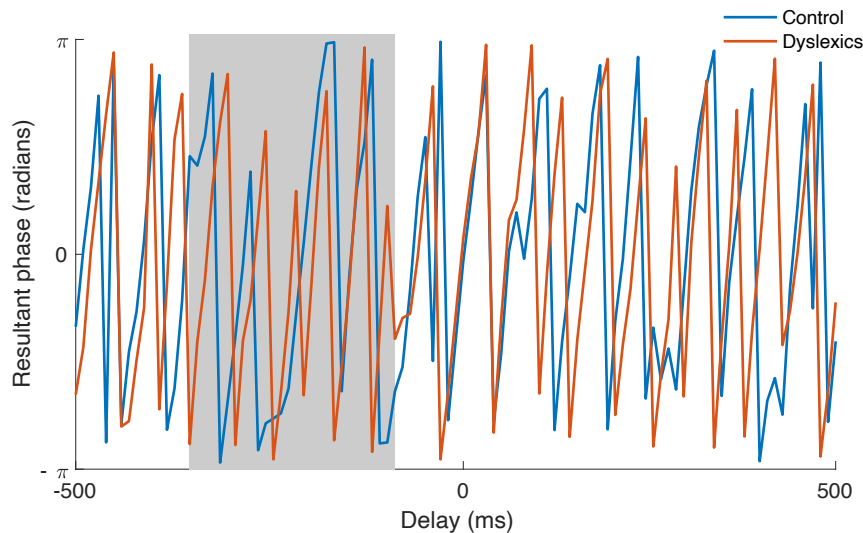
287 **Figure 2. Phase distribution across groups and group resultant vectors (red lines).** There is
288 significant phase entrainment across different children in the control group (panel A) but not in
289 the dyslexic group (Panel B). The length of the group resultant vector can be used as a criterion to
290 assess the strength of phase entrainment.

291

292 3.2. Comparing angular velocity between groups

293 To further assess the behaviour of preferred phase in the beta band for each group, we computed
294 angular velocity. Angular velocity is the rate of phase changes across time, providing an index of
295 pre-stimulus differences in phase just before the occurrence of the next “ba” syllable. *Group*
296 *angular velocity* was computed separately for each group in the entrainment period over the time

297 interval of -500 ms to 500 ms (relative to the occurrence of a stimulus, see Figure 3). Following
298 Keshavarzi et al.'s (2022a) report of a significant group difference in terms of pre-stimulus angular
299 velocity, we used two-sample t-tests to check for a group difference in terms of angular velocity
300 over different time intervals. The results showed that there was a significant difference in angular
301 velocity between the two groups over the time interval of -350 ms to -90 ms (controls: 34.2π
302 rad/s; children with dyslexia: 37.6π rad/s; two-sample t-test, $p = 0.008$). Accordingly, in the pre-
303 stimulus period, the rate of beta phase changes differs significantly between the two groups. These
304 changes were faster in the children with dyslexia.

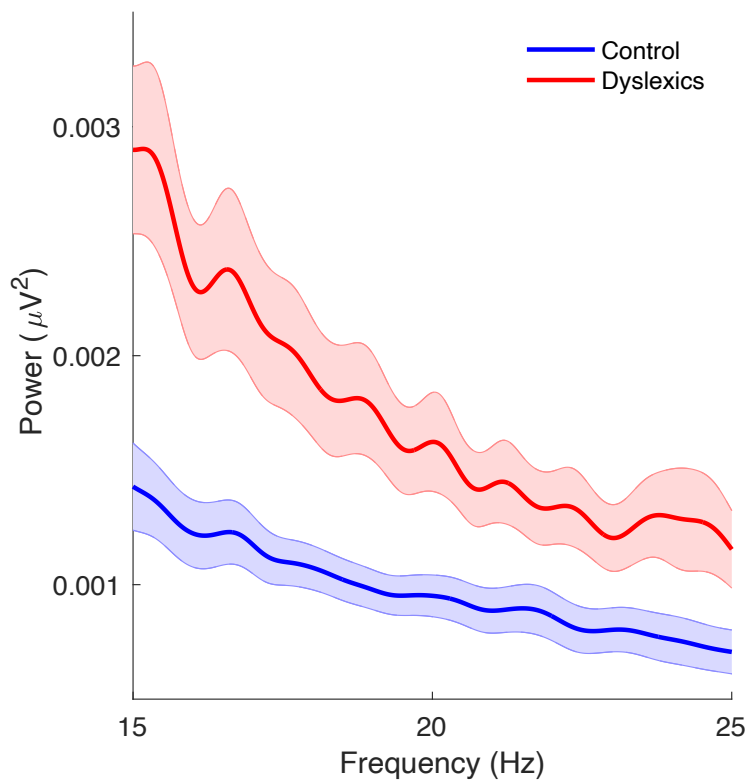


305
306 **Figure 3. The angular velocity (radians) versus the delay (ms) relative to “ba” stimuli onsets.**
307 The blue and red curves are for control and dyslexic groups, respectively.
308

309 3.3. Beta band power over the entrainment period (3 seconds)

310 To investigate the beta band power of neural response over the entrainment period used for analysis
311 (3 seconds), we calculated the power of EEG responses for each child and each group separately.
312 This was conducted in four steps: (1) Calculating the power of each EEG channel separately for
313 each trial; (2) Calculating the power for each trial by averaging across power values obtained (in
314 step 1) for channels; (3) Calculating the power for each child by averaging across power values

315 obtained (in step 2) for all trials of that child; (4) Calculating the power for each group by averaging
316 across power values obtained (in step 2) for all children in that group. Figure 4 demonstrates the
317 beta band power for each group. To compare average beta-band power for children in the control
318 group with those in the dyslexic group, we applied the Wilcoxon rank sum test after removing
319 outliers. Data points were treated as outliers if the corresponding power value was more than a 1.5
320 interquartile range above the upper quartile or below the lower quartile of the population data in
321 that group. There were 4 outliers in the dyslexic group and 3 outliers in the control group. The
322 results showed that beta band power obtained for the children with dyslexia was significantly
323 greater than that of control children (Wilcoxon rank sum test, $z = -2.42$, $p = 0.015$).



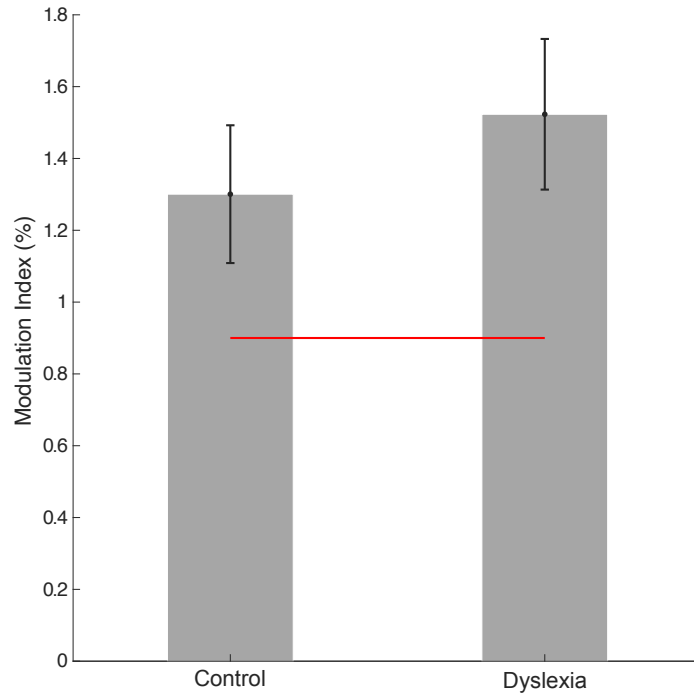
324
325 **Figure 4. Beta-band power.** The blue and red curves denote the power in the beta band versus
326 frequency for control and dyslexic groups, respectively. The shaded areas demonstrate the standard
327 error of the mean.

328
329
330
331
332
333
334
335
336
337
338
339
340
341
342
343
344
345
346

3.4. Delta-beta phase-amplitude coupling (PAC)

To study delta-beta PAC, the *MI* was computed separately for all trials of each child. The mean *MI* for a given child was then calculated by averaging across the *MI* scores obtained from the trials completed by that child. Figure 5 shows the mean *MI* scores for children in each group (control versus dyslexic). To compare *MI* between the two groups, a two-sample t-test was applied. No significant difference in PAC between the two groups was observed (Two-sample t-test, $p = 0.46$).

To assess whether the *MI* values obtained for dyslexic and control children were above chance, null models were computed. To this end, the EEG data corresponding to all 90 trials was first replaced by red noise (Hülsemann, 2019). We then calculated the *MI* separately for each trial using the procedure described in Subsection 2.8. We next computed the mean *MI* value by averaging across *MI* scores obtained for all 90 trials, resulting in one single score. This procedure was performed 1000 times, yielding 1000 scores. Chance level was obtained by averaging across these 1000 scores. To statistically compare *MI* scores obtained for children in the control group and in the dyslexic group with chance, we applied Wilcoxon rank sum tests separately. The results showed that *MI* scores obtained for both children with dyslexia and control children were statistically greater than chance (Wilcoxon rank sum test; control: $z = 5.61$, $p = 2 \times 10^{-8}$; dyslexia: $z = 8.1$, $p = 5 \times 10^{-16}$). Accordingly, significant delta-beta PAC was present in both groups.



347

348 **Figure 5. Modulation index as a measure of the strength of delta-beta phase-amplitude**
349 **coupling for control and dyslexic group.** The horizontal red line denotes the chance level.

350

351 4. Discussion

352 Here we set out to explore potential group differences in beta phase, beta power, angular velocity
353 and delta-beta PAC between children with and without dyslexia in response to rhythmic speech.

354 Given that prior studies with rhythmic speech as input have established atypical phase entrainment

355 in the delta band for children with dyslexia (Power et al., 2013; Keshavarzi et al., 2022a), and

356 given that delta phase modulates beta amplitude (through delta-beta PAC) during speech

357 processing for children (Power et al., 2016), it was expected that some atypical effects in the beta

358 band may also be present in those participants with developmental dyslexia. The data showed that

359 while significant phase entrainment in the beta band was present for the control children, the

360 children with dyslexia did not show significant phase entrainment in the beta band (Figure 2).

361 Accordingly, by the age of 9 years, the dyslexic brain has not yet established phase consistency in

362 the beta band when responding to rhythmic speech at 2 Hz. However, group angular velocity did
363 show a significant difference between groups. Group angular velocity over the time interval of –
364 500 ms to 500 ms (relative to the occurrence of a stimulus, see Figure 3) was investigated
365 separately for each group. There was a significant difference in angular velocity between the two
366 groups over the time interval of –350 ms to –90 ms (see Figure 3), indicative of faster changes in
367 beta phase in the children with dyslexia. Accordingly, beta phase in response to rhythmic input
368 does appear to be atypical in the dyslexic brain.

369 We also explored delta-beta PAC. PAC mechanisms are assumed to support the integration
370 (coordination) of processes in the brain (Mariscal et al., 2021), and delta-beta PAC has been
371 particularly studied with regard to temporal processing. Concerning rhythmic processing, Arnal et
372 al. (2014) have shown that oscillations in the delta and beta bands are instrumental in temporal
373 prediction in the adult brain, aligning with upcoming targets and supporting accurate behavioural
374 responding. Concerning speech processing, Pefkou et al. (2017) reported a role for endogenous
375 beta oscillations in speech comprehension by adults using a time-compressed speech paradigm.
376 Beta oscillations in the motor cortex contribute to planning movements, and Morillon et al. (2019)
377 showed functional delta-beta coupling during planned motor acts, which they argued may provide
378 a contextual temporal framework for processing slower linguistic information. In the current
379 rhythmic speech study, delta-beta PAC was found to be intact for the 9-year-old children with
380 dyslexia (see Figure 5). A similar result in a sentence listening paradigm was previously reported
381 for 14-year-old children with developmental dyslexia by Power et al. (2016). However, this finding
382 does not necessarily suggest that motor-based temporal prediction mechanisms in the dyslexic
383 brain are functioning efficiently. Indeed, it is known that children with dyslexia have difficulty in
384 tapping in time with a beat (Thomson and Goswami, 2008; Colling et al., 2017). In a reaction time

385 task based on rhythmic tones, adults with dyslexia do not show the same relation between faster
386 reaction times and the rising phase of the delta oscillation that is shown by non-dyslexic adults,
387 despite being matched for overall performance (Soltész et al., 2013). In adult studies, the entrained
388 delta-band phase-course has been thought to provide an internal “chronograph”, accurately
389 tracking elapsing time via the accumulation of phase information (Arnal and Kleinschmidt, 2017).
390 In particular, delta phase is known from adult studies to be important in detecting audio-visual
391 temporal asynchronies when prosodic information is manipulated (Biau et al., 2022). Children
392 with dyslexia have documented prosodic difficulties and show atypical delta phase (Goswami,
393 2022, for review), yet such prosodic temporal and motor paradigms have not yet been utilised with
394 children with dyslexia. Intriguingly, Biau et al. (2022) noted decreased delta-beta coupling in left
395 motor cortex when their adult participants could not accurately map visual and auditory prosodies.
396 It is thus possible that more naturalistic speech tasks than the rhythmic speech task employed here
397 could reveal some differences in delta-beta PAC in dyslexia.

398 Meanwhile, prior studies with participants with dyslexia have documented greater beta
399 power for both children with dyslexia (Klimesch et al., 2001; Spironelli et al., 2008) and adults
400 with dyslexia (Milne et al., 2003) during reading-related tasks. In the current speech listening
401 study, beta power in the dyslexic brain was significantly greater than beta power for the control
402 participants, replicating a finding previously reported by Power et al. (2016) for sentence listening
403 (see Figure 4). Beta-band power is known to be related to visual attention (Gola et al., 2013).
404 Accordingly, in the current audio-visual speech paradigm, greater beta band power in dyslexia
405 may serve as a compensatory mechanism for the impaired neural sampling of auditory information.
406 This could be investigated directly in future studies. Finally, although our task (listening to
407 syllables presented at a 2 Hz rate) is similar to the rhythmic task used by Chang et al. (2021) with

408 dyslexic adults (listening to tones presented at a 2 Hz rate), the main focus of our study was on the
409 phase entrainment of the neural responses in the beta band, and not on the phase of beta band
410 power fluctuation. As the children with dyslexia tested here did not show any phase consistency
411 in the beta band, we could not analyse the phase of beta band power fluctuations.

412 The current study has a number of limitations. Due to the Covid-19 Pandemic, the number
413 of control children was fewer than the number of children with dyslexia. Secondly, the paradigm
414 did not involve naturalistic continuous speech. Future studies with rhythmic tasks, ideally using
415 naturalistic speech paradigms such as the prosodic tasks devised by Biau et al. (2022), are required
416 in order to deepen our understanding of the potential role of beta oscillations in linguistic
417 processing for participants with dyslexia.

418 **Funding statement**

419 The research is funded by a grant awarded to UG by the Fondation Botnar (project number: 6064)
420 and a donation from the Yidan Prize Foundation. The sponsors had no role in the study design,
421 data analyses nor writing of the report.

422

423 **Ethics approval statement**

424 All participants and their parents gave informed consent for the EEG study in accordance with the
425 Declaration of Helsinki, and the study was reviewed by the Psychology Research Ethics
426 Committee of the University of Cambridge.

427

428 **Declaration of Competing Interest**

429 The authors declare no competing financial interests.

430

431 **Data availability**

432 Data will be made available on request.

433

434 **Acknowledgement**

435 The authors would like to thank Barbara Tillmann for first suggesting that we investigate beta
436 phase, and all the children, families and schools involved in the study.

437

438

439 References

- 440 Arnal, L.H., Doelling, K.B., Poeppel, D., 2015. Delta–beta coupled oscillations underlie temporal
441 prediction accuracy. *Cerebral Cortex*, 25(9), 3077-3085. <https://doi.org/10.1093/cercor/bhu103>.
- 442 Arnal, L.H., Giraud, A.L., 2012. Cortical oscillations and sensory predictions. *Trends in cognitive*
443 *sciences*, 16(7), 390-398. <https://doi.org/10.1016/j.tics.2012.05.003>.
- 444 Arnal, L.H., Kleinschmidt, A.K., 2017. Entrained delta oscillations reflect the subjective tracking
445 of time. *Communicative & integrative biology*, 10(5-6), 3077-3085.
446 <https://doi.org/10.1080/19420889.2017.1349583>.
- 447 Attaheri, A., Choidealbha, Á.N., Di Liberto, G.M., Rocha, S., Brusini, P., Mead, N., ..., Goswami,
448 U., 2022. Delta-and theta-band cortical tracking and phase-amplitude coupling to sung speech by
449 infants. *NeuroImage*, 247, 118698. <https://doi.org/10.1016/j.neuroimage.2021.118698>.
- 450 Attaheri, A., Ní Choidealbha, Á., Rocha, S., Brusini, P., Di Liberto, G.M., Mead, N., ..., Goswami,
451 U., 2022. Infant low-frequency EEG cortical power, cortical tracking and phase-amplitude
452 coupling predicts language a year later. *bioRxiv*. <https://doi.org/10.1101/2022.11.02.514963>.
- 453 Biau, E., Schultz, B.G., Gunter, T.C., Kotz, S.A., 2022. Left motor δ oscillations reflect
454 asynchrony detection in multisensory speech perception. *Journal of Neuroscience*, 42(11), 2313-
455 2326. <https://doi.org/10.1523/JNEUROSCI.2965-20.2022>.
- 456 Chang, A., Bedoin, N., Canette, L.H., Nozaradan, S., Thompson, D., Corneyllie, A., ..., Trainor,
457 L.J., 2021. Atypical beta power fluctuation while listening to an isochronous sequence in
458 dyslexia. *Clinical Neurophysiology*, 132(10), 2384-2390.
459 <https://doi.org/10.1016/j.clinph.2021.05.037>.
- 460 Colling, L.J., Noble, H.L., Goswami, U., 2017. Neural entrainment and sensorimotor
461 synchronization to the beat in children with developmental dyslexia: An EEG study. *Neuroscience*,
462 11, 360. <https://doi.org/10.3389/fnins.2017.00360>.
- 463 Delorme, A., Makeig, S., 2004. EEGLAB: an open source toolbox for analysis of single-trial EEG
464 dynamics including independent component analysis. *Journal of neuroscience methods*, 134(1),
465 9-21. <https://doi.org/10.1016/j.jneumeth.2003.10.009>.
- 466 Destoky, F., Bertels, J., Niesen, M., Wens, V., Vander Ghinst, M., Leybaert, J., ..., Bourguignon,
467 M., 2020. Cortical tracking of speech in noise accounts for reading strategies in children. *PLoS*
468 *biology*, 18(8), e3000840. <https://doi.org/10.1371/journal.pbio.3000840>.
- 469 Di Liberto, G.M., Peter, V., Kalashnikova, M., Goswami, U., Burnham, D., Lalor, E.C., 2018.
470 Atypical cortical entrainment to speech in the right hemisphere underpins phonemic deficits in
471 dyslexia. *NeuroImage*, 175, 70-79. <https://doi.org/10.1016/j.neuroimage.2018.03.072>.
- 472 Ding, N., Simon, J.Z., 2014. Cortical entrainment to continuous speech: functional roles and
473 interpretations. *Frontiers in human neuroscience*, 8, 311.
474 <https://doi.org/10.3389/fnhum.2014.00311>.
- 475 Doelling, K.B., Arnal, L.H., Ghitza, O., Poeppel, D., 2014. Acoustic landmarks drive delta–theta
476 oscillations to enable speech comprehension by facilitating perceptual parsing. *NeuroImage*, 85,
477 761-768. <https://doi.org/10.1016/j.neuroimage.2013.06.035>.

- 478 Elliott, C.D., Smith, P., McCulloch, K., 1996. British Ability Scales (2nd ed.). Windsor, UK:
479 NFER-Nelson.
- 480 Fiveash, A., Bedoin, N., Gordon, R.L., Tillmann, B., 2021. Processing rhythm in speech and
481 music: Shared mechanisms and implications for developmental speech and language
482 disorders. *Neuropsychology*, 35(8), 771. <https://doi.org/10.1037/neu0000766>.
- 483 Frederickson, N., Frith, U., Reason, R., 1997. *Phonological assessment battery (PhAB): Manual*
484 *and test materials*. NFER-Nelson.
- 485 Gisladottir, R.S., Bögels, S., Levinson, S.C., 2018. Oscillatory brain responses reflect anticipation
486 during comprehension of speech acts in spoken dialog. *Frontiers in human neuroscience*, 12, 34.
487 <https://doi.org/10.3389/fnhum.2018.00034>.
- 488 Gola, M., Magnuski, M., Szumska, I., Wróbel, A., 2013. EEG beta band activity is related to
489 attention and attentional deficits in the visual performance of elderly subjects. *International*
490 *Journal of Psychophysiology*, 89(3), 334-341. <https://doi.org/10.1016/j.ijpsycho.2013.05.007>.
- 491 Goswami, U., 2011. A temporal sampling framework for developmental dyslexia. *Trends in*
492 *cognitive sciences*, 15(1), 3-10. <https://doi.org/10.1016/j.tics.2010.10.001>.
- 493 Goswami, U., 2015. Sensory theories of developmental dyslexia: three challenges for
494 research. *Nature Reviews Neuroscience*, 16(1), 43-54. <https://doi.org/10.1038/nrn3836>.
- 495 Goswami, U., 2022. Language acquisition and speech rhythm patterns: an auditory neuroscience
496 perspective. *Royal Society Open Science*, 9(7), 211855. <https://doi.org/10.1098/rsos.211855>.
- 497 Greenberg, S., Carvey, H., Hitchcock, L., Chang, S., 2003. Temporal properties of spontaneous
498 speech—a syllable-centric perspective. *Journal of Phonetics*, 31(3-4), 465-485.
499 <https://doi.org/10.1016/j.wocn.2003.09.005>.
- 500 Gross, J., Hoogenboom, N., Thut, G., Schyns, P., Panzeri, S., Belin, P., Garrod, S., 2013. Speech
501 rhythms and multiplexed oscillatory sensory coding in the human brain. *PLoS biology*, 11(12),
502 e1001752. <https://doi.org/10.1371/journal.pbio.1001752>.
- 503 Hülsemann, M.J., Naumann, E., Rasch, B., 2019. Quantification of phase-amplitude coupling in
504 neuronal oscillations: comparison of phase-locking value, mean vector length, modulation index,
505 and generalized-linear-modeling-cross-frequency-coupling. *Frontiers in neuroscience*, 13, 573.
506 <https://doi.org/10.3389/fnins.2019.00573>.
- 507 Keitel, A., Gross, J., Kayser, C., 2018. Perceptually relevant speech tracking in auditory and motor
508 cortex reflects distinct linguistic features. *PLoS biology*, 16(3), e2004473.
509 <https://doi.org/10.1371/journal.pbio.2004473>.
- 510 Keshavarzi, M., Mandke, K., Macfarlane, A., Parvez, L., Gabrielczyk, F., Wilson, A., Goswami,
511 U., 2022a. Atypical delta-band phase consistency and atypical preferred phase in children with
512 dyslexia during neural entrainment to rhythmic audio-visual speech. *NeuroImage: Clinical*, 35,
513 103054. <https://doi.org/10.1016/j.nicl.2022.103054>.
- 514 Keshavarzi, M., Mandke, K., Macfarlane, A., Parvez, L., Gabrielczyk, F., Wilson, A., ...,
515 Goswami, U., 2022b. Decoding of speech information using EEG in children with dyslexia: Less
516 accurate low-frequency representations of speech, not “Noisy” representations. *Brain and*
517 *Language*, 235, 105198. <https://doi.org/10.1016/j.bandl.2022.105198>.

- 518 Klimesch, W., Doppelmayr, M., Wimmer, H., Gruber, W., Röhms, D., Schwaiger, J., Hutzler, F.,
519 2001. Alpha and beta band power changes in normal and dyslexic children. *Clinical*
520 *Neurophysiology*, 112(7), 1186-1195. [https://doi.org/10.1016/s1388-2457\(01\)00543-0](https://doi.org/10.1016/s1388-2457(01)00543-0).
- 521 Ladányi, E., Persici, V., Fiveash, A., Tillmann, B., Gordon, R.L., 2020. Is atypical rhythm a risk
522 factor for developmental speech and language disorders?. *Wiley Interdisciplinary Reviews:*
523 *Cognitive Science*, 11(5), e1528. <https://doi.org/10.1002/wcs.1528>.
- 524 Levitt, H.C.C.H., 1971. Transformed up-down methods in psychoacoustics. *The Journal of the*
525 *Acoustical society of America*, 49(2B), 467-477. <https://doi.org/10.1121/1.1912375>.
- 526 Mandke, K., Flanagan, S., Macfarlane, A., Gabrielczyk, F., Wilson, A., Gross, J., Goswami, U.,
527 2022. Neural sampling of the speech signal at different timescales by children with
528 dyslexia. *NeuroImage*, 253, 119077. <https://doi.org/10.1016/j.neuroimage.2022.119077>.
- 529 Meng, X., Sun, C., Du, B., Liu, L., Zhang, Y., Dong, Q., ..., Nan, Y., 2022. The development of
530 brain rhythms at rest and its impact on vocabulary acquisition. *Developmental science*, 25(2),
531 e13157. <https://doi.org/10.1111/desc.13157>.
- 532 Milne, R.D., Hamm, J.P., Kirk, I.J., Corballis, M.C., 2003. Anterior-posterior beta asymmetries
533 in dyslexia during lexical decisions. *Brain and Language*, 84(3), 309-317.
534 [https://doi.org/10.1016/s0093-934x\(02\)00557-6](https://doi.org/10.1016/s0093-934x(02)00557-6).
- 535 Leong, V., Goswami, U., 2015. Acoustic-emergent phonology in the amplitude envelope of child-
536 directed speech. *PloS One*, 10(12), e0144411. <https://doi.org/10.1371/journal.pone.0144411>.
- 537 Leong, V., Kalashnikova, M., Burnham, D., Goswami, U., 2017. The temporal modulation
538 structure of infant-directed speech. *Open Mind*, 1(2), 78-90.
539 https://doi.org/10.1162/OPMI_a_00008.
- 540 Mariscal, M.G., Levin, A.R., Gabard-Durnam, L.J., Xie, W., Tager-Flusberg, H., Nelson, C.A.,
541 2021. EEG phase-amplitude coupling strength and phase preference: association with age over the
542 first three years after birth. *Eneuro*, 8(3). <https://doi.org/10.1523/eneuro.0264-20.2021>.
- 543 Mehler, J., Jusczyk, P., Lambertz, G., Halsted, N., Bertoni, J., Amiel-Tison, C., 1988. A
544 precursor of language acquisition in young infants. *Cognition*, 29(2), 143-178.
545 [https://doi.org/10.1016/0010-0277\(88\)90035-2](https://doi.org/10.1016/0010-0277(88)90035-2).
- 546 Molinaro, N., Lizarazu, M., Lallier, M., Bourguignon, M., Carreiras, M., 2016. Out-of-synchrony
547 speech entrainment in developmental dyslexia. *Human brain mapping*, 37(8), 2767-2783.
548 <https://doi.org/10.1002/hbm.23206>.
- 549 Morillon, B., Arnal, L.H., Schroeder, C.E., Keitel, A., 2019. Prominence of delta oscillatory
550 rhythms in the motor cortex and their relevance for auditory and speech perception. *Neuroscience*
551 *& Biobehavioral Reviews*, 107, 136-142. <https://doi.org/10.1016/j.neubiorev.2019.09.012>.
- 552 Nazzi, T., Bertoni, J., Mehler, J., 1998. Language discrimination by newborns: toward an
553 understanding of the role of rhythm. *Journal of Experimental Psychology: Human perception and*
554 *performance*, 24(3), 756. <https://doi.org/10.1037//0096-1523.24.3.756>.
- 555 Pefkou, M., Arnal, L.H., Fontolan, L., Giraud, A.L., 2017. θ -Band and β -band neural activity
556 reflects independent syllable tracking and comprehension of time-compressed speech. *Journal of*
557 *Neuroscience*, 37(33), 7930-7938. <https://doi.org/10.1523/jneurosci.2882-16.2017>.

- 558 Power, A.J., Colling, L.J., Mead, N., Barnes, L., Goswami, U., 2016. Neural encoding of the
559 speech envelope by children with developmental dyslexia. *Brain and Language*, 160, 1-10.
560 <https://doi.org/10.1016/j.bandl.2016.06.006>.
- 561 Power, A.J., Mead, N., Barnes, L., Goswami, U., 2012. Neural entrainment to rhythmically
562 presented auditory, visual, and audio-visual speech in children. *Frontiers in Psychology*, 3, 216.
563 <https://doi.org/10.3389/fpsyg.2012.00216>.
- 564 Power, A.J., Mead, N., Barnes, L., Goswami, U., 2013. Neural entrainment to rhythmic speech in
565 children with developmental dyslexia. *Frontiers in human neuroscience*, 7, 777.
566 <https://doi.org/10.3389/fnhum.2013.00777>.
- 567 Soltész, F., Szűcs, D., Leong, V., White, S., Goswami, U., 2013. Differential entrainment of
568 neuroelectric delta oscillations in developmental dyslexia. *PloS One*, 8(10), Article e76608.
569 <https://doi.org/10.1371/journal.pone.0076608>.
- 570 Spironelli, C., Penolazzi, B., Angrilli, A., 2008. Dysfunctional hemispheric asymmetry of theta
571 and beta EEG activity during linguistic tasks in developmental dyslexia. *Biological*
572 *psychology*, 77(2), 123-131. <https://doi.org/10.1016/j.biopsycho.2007.09.009>.
- 573 Thomson, J.M., Goswami, U., 2008. Rhythmic processing in children with developmental
574 dyslexia: Auditory and motor rhythms link to reading and spelling. *Journal of Physiology- Paris*,
575 102, 120-129. <https://doi.org/10.1016/j.biopsycho.2007.09.009>.
- 576 Torgesen, J., Wagner, R.K., Rashotte, C., 1999. Test of Word Reading Efficiency (TOWRE).
577 Austin, TX: Pro-Ed.
- 578 Tort, A.B., Kramer, M.A., Thorn, C., Gibson, D.J., Kubota, Y., Graybiel, A.M., Kopell, N.J., 2008.
579 Dynamic cross-frequency couplings of local field potential oscillations in rat striatum and
580 hippocampus during performance of a T-maze task. *Proceedings of the National Academy of*
581 *Sciences*, 105(51), 20517-20522. <https://doi.org/10.1073/pnas.0810524105>.